

Bridging Polymeric Turbulence at different Reynolds numbers: From Multiscaling to Multifractality

Rahul K. Singh^{1,*} and Marco E. Rosti^{1,†}

¹*Complex Fluids and Flows Unit, Okinawa Institute of Science and Technology Graduate University, Okinawa 904-0495, Japan*

The addition of polymers modifies a flow in a non-trivial way that depends on fluid inertia (given by the Reynolds number Re) and polymer elasticity (quantified by the Deborah number De). Using direct numerical simulations, we show that polymeric flows exhibit a Re and De dependent multiscaling energy spectrum. The different scaling regimes are tied to various dominant contributions—fluid, polymer, and dissipation—to the total energy flux across the scales. At small scales, energy is dissipated away by both polymers and the fluid. Fluid energy dissipation, in particular, is shown to be more intermittent in the presence of polymers, especially at small Re . The more intermittent, singular nature of energy dissipation is revealed clearly by the multifractal spectrum.

Polymeric flows give rise to a wide range of intriguing phenomena. The earliest known example is of turbulent drag reduction due to small polymer concentrations [1–3], which inspired a number of numerical [4–9] and theoretical studies [10–12]. Polymers tend to increase the effective viscosity of a solution [2, 13], however there can be a net reduction in energy dissipation in turbulent flows [5, 6, 14–16]. Small Reynolds number (Re) flows, which are smooth, predictable, and laminar, are very well known to develop instabilities in the presence of polymers [17–20], leading to elastic turbulence (ET). ET is marked by a chaotic flow regime [21–23], enhanced mixing [24], and a self-similar distribution of kinetic energy across a wide range of scales [25–27]. At moderate Re , polymer elasticity (characterised by Deborah number De) and fluid inertia (Re) conspire to trigger a turbulence-like behaviour much earlier than in a Newtonian flow [28–31] and is referred to as elasto-inertial turbulence (EIT). Fluid kinetic energy in EIT also shows a distinct scaling behaviour [28, 30, 32]. Finally, high Re polymeric, homogeneous, isotropic, turbulent (PHIT) flows have been recently shown to modify the scaling exponents predicted by the Kolmogorov theory (K41) [33, 34] via both experiments [35] and simulations [36].

Majority of these earlier studies have focused largely on a small range of Re and De numbers. However, a complete understanding of how various flow characteristics depend on fluid inertia (Re) and polymer elasticity (De) still remains evasive. We address this issue in the current work by spanning a decade in both Re and De numbers. This becomes even more critical in light of some recent results. First, PHIT [35, 36] and ET [32, 37], being phenomena at very different Re numbers, show very different self-similarity of energy spectrum. Second, intermittency of energy dissipation in PHIT is identical to classical, homogeneous, isotropic turbulence (HIT) [36], but is again different from that in ET [37]. This immediately raises

the question: *What happens to the distribution, and ultimately dissipation of kinetic energy in polymeric flows at intermediate Re ? And how does elasticity help shape this landscape of polymeric turbulence?*

We address these questions via the direct numerical simulations of polymeric flows comprising an incompressible fluid velocity field \mathbf{u} ($\nabla \cdot \mathbf{u} = 0$), and a polymer conformation tensor field \mathbf{C} , whose trace C_{ii} , $i = 1, 2, 3$, is a measure of the averaged squared lengths of the polymers. To this end, we adopt the Oldroyd-B model of polymers, which has often been used to study polymeric flows in various settings [25, 27, 32, 38–40]. The flow evolution is given by the coupled equations:

$$\rho (\partial_t \mathbf{u} + \mathbf{u} \cdot \nabla \mathbf{u}) = -\nabla p + \mu_s \nabla^2 \mathbf{u} + \frac{\mu_p}{\tau_p} \nabla \cdot \mathbf{C} + \mathbf{F}, \quad (1a)$$

$$\partial_t \mathbf{C} + \mathbf{u} \cdot \nabla \mathbf{C} = \mathbf{C} \nabla \mathbf{u} + (\nabla \mathbf{u})^T \mathbf{C} - \frac{1}{\tau_p} (\mathbf{C} - \mathbf{I}), \quad (1b)$$

where p is the pressure, ρ the fluid density, μ_s the dynamic viscosity of the Newtonian fluid (kinematic viscosity $\nu = \mu_s/\rho$), μ_p the dynamic polymer viscosity, and τ_p is the unique relaxation time of the polymers. A statistically stationary state is maintained by energy injection via the forcing \mathbf{F} [41]. The total energy injected per unit time ϵ_t is dissipated away by both the Newtonian fluid (ϵ_f) and the polymers (ϵ_p), $\epsilon_t = \epsilon_f + \epsilon_p$. The flow is characterised by two dimensionless numbers: the Taylor-scale Reynolds number, $Re_\lambda \equiv u_{rms} \lambda / \nu$, where $\lambda \equiv u_{rms} \sqrt{15\nu/\epsilon_f}$ is the Taylor length scale and u_{rms} the root mean square velocity, and the Deborah number, $De \equiv \tau_p / \tau_L$, where $\tau_L = L/u_{rms}$ is the large-eddy turnover time, with L being the scale of the forcing. We choose $Re_\lambda \in \{40, 100, 240, 320, 460\}$ and $De \in \{1/9, 1/3, 1, 3, 9\}$. Lastly, we fix fluid and polymer viscosities such that $\mu_s / (\mu_s + \mu_p) = 0.9$ [42]. We show representative, two-dimensional slices of ϵ_f -fields in Fig. 1 for $Re_\lambda \approx 460$ in panel (a) and $Re_\lambda \approx 40$ in panel (b).

We begin by showing how fluid kinetic energy is distributed across scales k in Fig. 1 (c, d). The spectrum $E(k)$ is a measure of the kinetic energy per mode such that the total energy $\mathcal{E} = \langle |\mathbf{u}|^2 \rangle / 2 = \int E(k) dk$. We recall

* rksphys@gmail.com

† marco.rosti@oist.jp

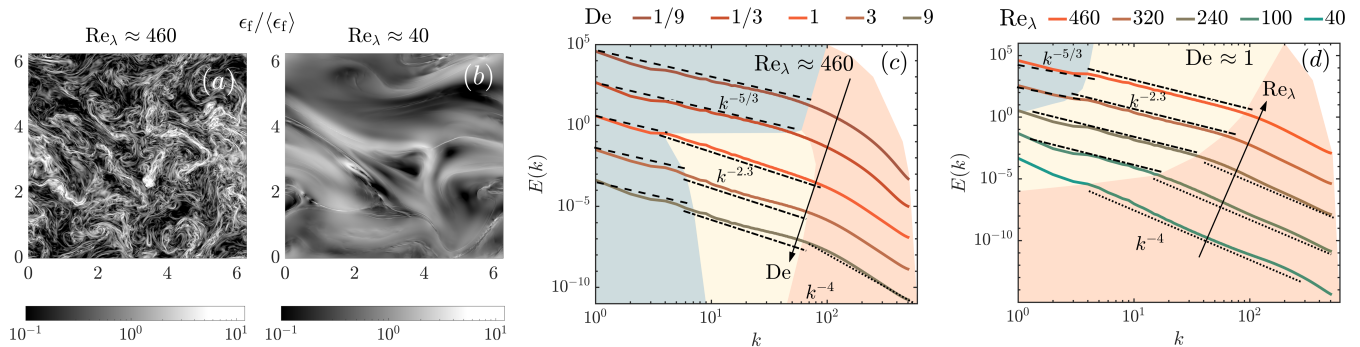


FIG. 1. (a and b) Normalized fluid dissipation rates ϵ_f at (a) large and (b) small Re when $\text{De} \approx 1$. (c and d) Multiscaling of $E(k)$ in polymeric flows at different (c) De and (d) Re numbers. Three distinct scaling regimes (in different shades) have been shown in dashed ($k^{-5/3}$, Newtonian), dash-dotted ($k^{-2.3}$, polymeric) and dotted ($k^{-\gamma}$; $\gamma \geq 4$, smooth) lines. (c) All three regimes can be seen clearly when $\text{De} \approx 1$. At smaller De , the behaviour is very close to Newtonian and at large De the largest scales again show a shift towards the Newtonian scaling. (d) The triple scaling at largest Re gives way to dual scaling at intermediate Re as the Newtonian regime vanishes. The smallest Re shows only the smooth k^{-4} range.

that $E(k) \sim k^{-5/3}$ in the inertial range of HIT [33, 34] which is modified to $E(k) \sim k^{-2.3}$ in PHIT [35, 36], while ET shows $E(k) \sim k^{-4}$ [37]. We now show that polymeric flows, in fact, exhibit a multi-scaling behaviour.

The different scaling regimes are shown in different shades in Fig. 1. Panel (c) shows how the spectrum changes with De at large Re . At small De , i.e. in the limit $\tau_p \rightarrow 0$, polymers stretch minimally as $\mathbf{C} \approx \mathbf{I}$ from Eqn. 1b. Thus, fluctuations in \mathbf{C} are minimal so that $\nabla \cdot \mathbf{C} \approx 0$, and the Navier-Stokes' equations are recovered from Eq. 1a. Consequently, the classical K41 result $E(k) \sim k^{-5/3}$ holds. As De is increased, polymers stretch to much longer lengths and the stress contributions become non-negligible. The interplay of inertia and elasticity over a wide range of scales then results in a multi-scaling energy spectrum, especially for $\text{De} \approx 1$. This is seen in the three distinct scaling regimes where $E(k) \sim k^{-\delta}$, with $\delta = 5/3 \forall k \leq 4$ (Newtonian regime at large scales), $\delta = 2.3 \forall k \in [4, 60]$ (polymeric regime at intermediate scales), and $\delta \geq 4 \forall k > 60$ (smooth at small scales). At yet larger De ($\approx 3, 9$), the polymeric range shrinks while the Newtonian range begins to extend again, finally recovering the $-5/3$ scaling in the large De limit [36]. Of course, polymers with very large relaxation times cannot follow the carrier flow, and essentially decouple from it (seeing it only as background noise). Thus, in the stationary state, the polymer stress contributions becomes small as $\tau_p \rightarrow \infty$, and the Newtonian scaling is recovered again for large De [36]. Thus, $\text{De} \approx 1$ results in an extended multiscaling behaviour.

But does the multiscaling picture still hold at small Re ? Our simulations definitely suggest so, albeit not without modifications. We plot $E(k)$ at different Re for $\text{De} \approx 1$ in Fig. 1(d). As Re decreases, fluid non-linearities become less important and the Newtonian range first shrinks and then disappears. The large scales now show the polymer scaling $E(k) \sim k^{-2.3}$. Moreover, the smooth range at

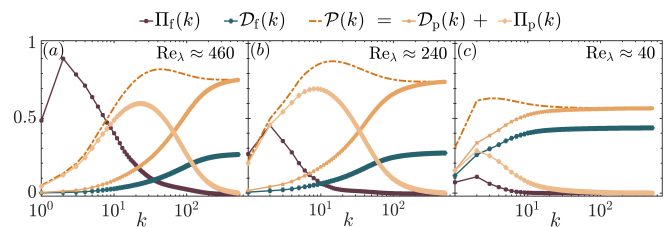


FIG. 2. Normalized flux contributions at (a) $\text{Re}_\lambda \approx 460$, (b) 240, and (c) 40 for flows with $\text{De} \approx 1$. (a) At large Re_λ , three distinct regimes are determined by different dominant contributions: large scales are dominated by the fluid non-linear flux Π_f , intermediate scales by the polymer flux Π_p , and small scales by the polymer dissipation \mathcal{D}_p . (b) Moderate Re_λ comprises two distinct regimes dominated by Π_p and \mathcal{D}_p . (c) When Re_λ is small, only dissipative terms remain important.

small scales also widens. Thus, at moderate $\text{Re}_\lambda \approx 240$, polymeric flows show a dual scaling of the energy spectrum so that $E(k) \sim k^{-\delta}$ where $\delta = 2.3$ for $k \lesssim 40$ and $\delta > 4$ for $k > 40$. At very small $\text{Re}_\lambda \approx 40$, an extended, unique k^{-4} scaling marks ET for $\text{De} \gtrsim 1$ [37].

The co-existence of various scaling regimes can be better understood by looking at the dominant energy transfer mechanisms across scales. To this end, we compute energy flux contributions from various terms in Eqn. 1a [42]. The rate of energy transfer from scales $< K$ to those $> K$ can be computed in a normalised form as $\Pi_f(K) + \mathcal{D}_f(K) + \mathcal{P}(K) = 1$ [42], where Π_f , \mathcal{D}_f , and, \mathcal{P} are the (negative) contributions from the non-linear, viscous, and polymeric terms respectively.

Following [36], we partition the polymeric contribution into flux (Π_p) and dissipative (\mathcal{D}_p) terms: $\mathcal{P}(K) = \Pi_p(K) + \mathcal{D}_p(K)$, where $\mathcal{D}_p(K) \equiv (\epsilon_p/\epsilon_f)\mathcal{D}_f(K)$. We show various flux contributions for $\text{De} \approx 1$ at different Re in Fig. 2. We indeed see from panel (a) that a dominant non-linear flux Π_f gives the $k^{-5/3}$ scaling at large scales

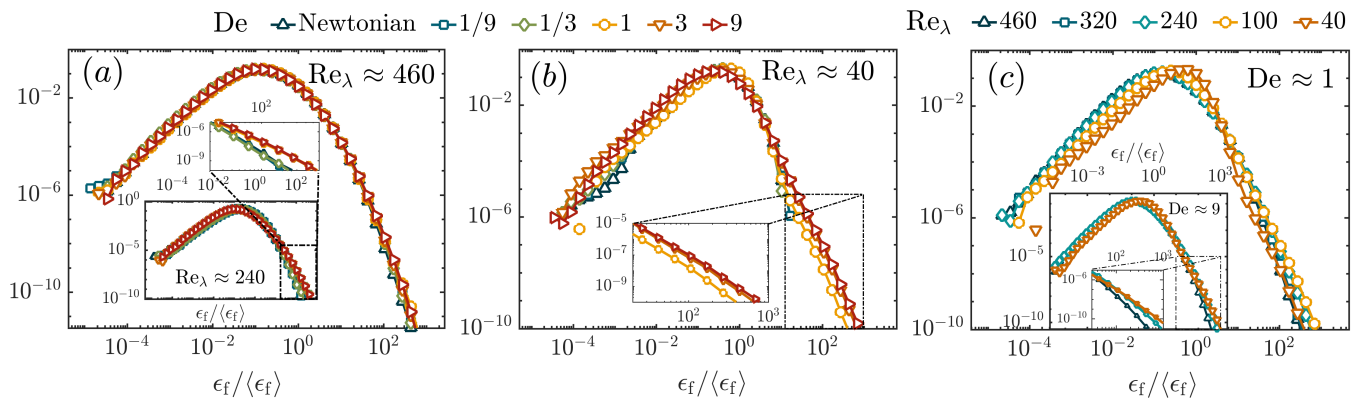


FIG. 3. Pdfs of the fluid energy dissipation rate ϵ_f . (a) Log-log plots of the pdfs at $\text{Re}_\lambda \approx 460$ (240) in the main (inset) for various De . Dissipation at large Re is unaffected by polymers, while at smaller Re , large De polymers result in wider right tails (see zoom of inset). (b) At $\text{Re}_\lambda \approx 40$, ET develops only for $\text{De} \gtrsim 1$ [37] and is marked by intermittent dissipation. Notice the absent right tails for $\text{De} < 1$ in the inset. (c) The left tails of ϵ_f -pdfs shrink as Re is reduced, similar to that in HIT [43]. The right tails, however, widen with decreasing Re (see inset when $\text{De} \approx 9$), contrary to that in HIT [43].

($k \leq 4$) (see Fig. 1(d)). Beyond this range, a dominant polymeric flux Π_p results in the polymeric range upto $k \approx 60$. At yet smaller scales, fluid (\mathcal{D}_f) and polymer (\mathcal{D}_p) dissipation remove energy from the flow rapidly, giving a faster than k^{-4} decay of the spectrum. Now, as Re_λ is decreased to moderate values (≈ 240) in Fig. 2(b), fluid non-linear interactions (Π_f) become weaker and energy flux at the largest scales is dictated by Π_p . Moreover, an increase in viscosity also means that dissipative contributions become important at relatively smaller k , consistent with a wider k^{-4} regime in Fig. 1(d). Finally, for very small $\text{Re}_\lambda \approx 40$ in Fig. 2(c), \mathcal{D}_p and \mathcal{D}_f are always larger than both Π_p and Π_f so that energy is now removed by viscosity even from the largest scales, giving the extended k^{-4} range in Fig. 1(d).

The scaling behaviour of $E(k)$, additionally, allows us to estimate the scaling behaviour of the polymer spectrum $E_p(k)$. Using both scaling arguments and simulations, we show $E_{pk} \sim k^{-1.35}$ for large Re and $E_{pk} \sim k^{-3/2}$ for small Re [42].

How is this energy, then, dissipated away by our polymeric fluids at the smallest scales? And how does this differ from dissipation in HIT, if at all? These questions are best answered via the statistics of fluid energy dissipation rate $\epsilon_f = 2\nu S_{ij}S_{ij}$, where $S_{ij} = (\partial_i u_j + \partial_j u_i)/2$ is the rate-of-strain tensor. We recall that ϵ_f in HIT is strongly intermittent and its distribution has stretched exponential tails [43–45]. We now show probability distribution functions (pdfs) of ϵ_f for different Re and De in Fig. 3. At large Re , polymers do not affect the statistics of ϵ_f and the pdfs for different De collapse in Fig. 3(a). This is because polymer stress contributions are sub-dominant compared to fluid non-linearities [42]. At moderate $\text{Re}_\lambda \approx 240$, the pdfs begin to depart at the right tails for large De as seen in the zoomed right tails of the inset in Fig. 3(a). Polymeric contributions,

for large elasticity, no longer remain small compared to fluid non-linearities and can create strong gradients in the flow. This effect is even more accentuated at the smallest $\text{Re}_\lambda \approx 40$ in Fig. 3(b), where the pdfs develop right-tails only for $\text{De} \gtrsim 1$. For Newtonian (and small De) flows at such small Re_λ , dissipation is devoid of extreme, intermittent events, resulting in the absent right tails (see zoomed inset). This is because small De polymers do not undergo coil-stretch transition and are unable to create strong fluctuations in the flow. However, at large De , the continuous stretching and relaxation of polymers creates strong fluctuations in the flow which results in large gradients in the flow [42]. This results in extreme events of dissipation, and gives the pdfs their characteristic long tails in Fig. 3(b) at large De . We substantiate these arguments in the Supplementary Material [42].

The main (inset) panel of Fig. 3(c) shows how dissipation pdfs change with Re_λ for $\text{De} \approx 1$ (9). The left tails shrink as Re_λ decreases, similar to what was recently noted in HIT [43]. However, the right tails of the ϵ_f -pdfs in polymeric flows show a trend contrary to HIT, as the right tails widen ever so slightly when Re is decreased [46]. Evidently, highly elastic polymers make dissipation more intermittent when Re_λ is small. This is seen more clearly in the zoomed tails in the inset when $\text{De} \approx 9$.

The changing right tails of ϵ_f -pdfs indicate that intermittency is a function of Re_λ and De . An intermittent dissipation field is non-space filling: some regions dissipate more than others. This means that moments of ϵ_f depend on the scale of averaging. The multifractal description of turbulence states that dissipation, in fact, accumulates on a continuum of fractal subsets [34]. Each of these fractals lends its contribution to a distinct moment q of $\langle \epsilon_f \rangle$, such that $\langle \epsilon_{f,l}^q \rangle \sim l^{\tau_q}$, where $q, \tau_q \in \mathbb{R}$ and subscript l denotes averaging over a cube of size l [34, 47–52].

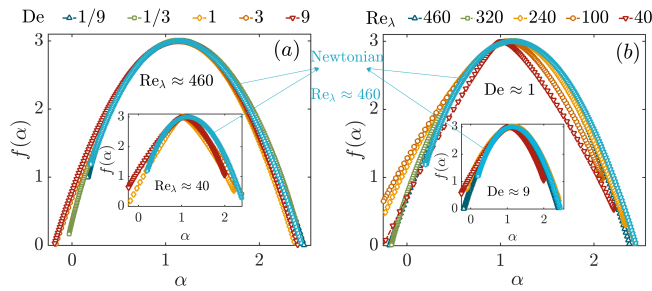


FIG. 4. The multifractal $f(\alpha)$ - α spectra for polymeric flows at (a) $Re_\lambda \approx 460$ (240) shown in the main (inset). Spectra at large Re coincide with that of HIT (shown in light blue in all panels). (b) Spectra at different Re for $De \approx 1$ (main) and $De \approx 9$ (inset). The spectrum widens as Re increases, while changing polymer elasticity at high Re has a minimal effect on the multifractality of the dissipation field.

The exponent τ_q is then related to the dimension $f(\alpha)$ of the contributing fractal via a Legendre transform [34, 48–50]:

$$\tau_q = \min_{\alpha} [q(\alpha - 1) + 3 - f(\alpha)], \quad (2)$$

and α determines how singular is the dissipation field: $\langle \epsilon_{f,l} \rangle \sim l^{\alpha-1}$ as $l \rightarrow 0$ [34, 47, 48]. The $f(\alpha)$ - α multifractal spectra thus computed are shown in Fig. 4 and are compared to that of HIT (shown in light blue colour in all panels). We show the spectra for varying De in Fig. 4(a) and for different Re in Fig. 4(b). The $f(\alpha)$ curves remain independent of De at large Re_λ , and coincide with that of HIT in 4(a, main), consistent with recent observations [36]. However, for small Re_λ in the inset, the fractal spectra deviate from that of HIT 4(a), but tend to the same curve at large De , suggesting universality [37]. The shrunk right and wider left branches of the spectra indicate that dissipation is more singular in ET (compared to HIT) when dissolved polymers have large elasticity. This is because dissipation $\langle \epsilon_{f,l} \rangle \sim l^{\alpha-1}$ is much stronger in regions where α is small as $l \rightarrow 0$, which is indicative of its more singular, intermittent nature. Between these two extremes of PHIT and ET, the spectra in Fig. 4(b) suggest an increasingly more singular behaviour with decreasing Re_λ for $De \approx 1$ as they become more and more skewed towards small α (inset shows the same for $De \approx 9$). Clearly, the addition of polymers makes the dissipation field more intermittent with decreasing Re_λ .

In this work, we have shown that polymeric flows admit a multi-scaling behaviour which is a function of both Re and De . This is most clearly seen for large Re and $De \approx 1$, so that $E(k) \sim k^\delta$ with:

$$\delta \begin{cases} = -5/3, & k \text{ small,} \\ = -2.3, & k \text{ intermediate,} \\ < -4, & k \text{ large.} \end{cases} \quad (3)$$

With decreasing Re , the $-5/3$ range disappears and the

spectrum shows a -2.3 power-law at large scales followed by a < -4 scaling exponent at small scales. This ultimately gives way to ET at small Re with a unique scaling exponent $\delta = -4$ [37]. The various scaling regimes, of course, result from different dominant contributions to the energy flux to small scales.

Unlike the energy spectrum [6, 35, 36, 53–60], dissipation in polymeric flows has been far less studied [36, 61, 62]. In this work, we show that dissipation in polymeric flows is not only intermittent, but also has a qualitatively similar distribution as in HIT. The distinction in the intermittent effects is unravelled by the multifractal spectrum: energy dissipation is, on an average, more singular in polymeric flows, and more so at small Re and large De . A more local quantification of the fractal spectrum may help shed more light into the nature of intermittent dissipation in polymeric flows in general, and ET in particular [63].

Our work not only provides crucial insights into how various turbulence characteristics depend on both Re and De , but also lends a fresh impetus into more detailed investigations of (turbulent) polymeric flows. All of the results discussed are easily testable by experiments, and can prove to be pivotal in a better understanding of turbulence in polymeric flows.

ACKNOWLEDGMENTS

The research was supported by the Okinawa Institute of Science and Technology Graduate University (OIST) with subsidy funding from the Cabinet Office, Government of Japan. The authors acknowledge the computer time provided by HPCI under the grants hp210229, hp210269 and hp220099, and by the Scientific Computing section of Research Support Division at OIST. The authors thank Prof. Dhruv Mitra and Prof. Prasad Perlekar for various useful discussions. R.K.S. thanks Alessandro Chiarini (OIST) for discussions and suggestions.

-
- [1] Toms B. A., “Some observations on the flow of linear polymer solutions through straight tubes at large reynolds numbers,” *Proc. 1st Int. Cong. Rheology, Amsterdam, 1948* **135** (1948).
 - [2] J. L. Lumley, “Drag reduction in turbulent flow by polymer additives,” *Journal of Polymer Science: Macromolecular Reviews* **7**, 263–290 (1973).
 - [3] B. A. Toms, “On the early experiments on drag reduction by polymers,” *The Physics of Fluids* **20**, S3–S5 (1977).
 - [4] Roberto Benzi, Elisabetta De Angelis, Rama Govindarajan, and Itamar Procaccia, “Shell model for drag reduction with polymer additives in homogeneous turbulence,” *Phys. Rev. E* **68**, 016308 (2003).
 - [5] Chirag Kalelkar, Rama Govindarajan, and Rahul Pan-

- dit, “Drag reduction by polymer additives in decaying turbulence,” *Phys. Rev. E* **72**, 017301 (2005).
- [6] Prasad Perlekar, Dhruvaditya Mitra, and Rahul Pandit, “Manifestations of drag reduction by polymer additives in decaying, homogeneous, isotropic turbulence,” *Phys. Rev. Lett.* **97**, 264501 (2006).
- [7] Christopher M. White and M Godfrey Mungal, “Mechanics and prediction of turbulent drag reduction with polymer additives,” *Annual Review of Fluid Mechanics* **40**, 235–256 (2008).
- [8] George H. Choueiri, Jose M. Lopez, and Björn Hof, “Exceeding the asymptotic limit of polymer drag reduction,” *Phys. Rev. Lett.* **120**, 124501 (2018).
- [9] Li Xi, “Turbulent drag reduction by polymer additives: Fundamentals and recent advances,” *Physics of Fluids* **31** (2019), 10.1063/1.5129619.
- [10] K. R. Sreenivasan and C. M. White, “The onset of drag reduction by dilute polymer additives, and the maximum drag reduction asymptote,” *Journal of Fluid Mechanics* **409**, 149–164 (2000).
- [11] M. Tabor and P. G. de Gennes, “A cascade theory of drag reduction,” *Europhysics Letters* **2**, 519 (1986).
- [12] Itamar Procaccia, Victor S. L’vov, and Roberto Benzi, “Colloquium: Theory of drag reduction by polymers in wall-bounded turbulence,” *Rev. Mod. Phys.* **80**, 225–247 (2008).
- [13] E. J. Hinch, “Mechanical models of dilute polymer solutions in strong flows,” *The Physics of Fluids* **20**, S22–S30 (1977).
- [14] Eric van Doorn, Christopher M. White, and K. R. Sreenivasan, “The decay of grid turbulence in polymer and surfactant solutions,” *Physics of Fluids* **11**, 2387–2393 (1999).
- [15] Prasad Perlekar, Dhruvaditya Mitra, and Rahul Pandit, “Direct numerical simulations of statistically steady, homogeneous, isotropic fluid turbulence with polymer additives,” *Phys. Rev. E* **82**, 066313 (2010).
- [16] W.-H. Cai, F.-C. Li, and H.-N. Zhang, “Dns study of decaying homogeneous isotropic turbulence with polymer additives,” *Journal of Fluid Mechanics* **665**, 334–356 (2010).
- [17] E S G Shaqfeh, “Purely elastic instabilities in viscometric flows,” *Annual Review of Fluid Mechanics* **28**, 129–185 (1996).
- [18] R. G. Larson, “Instabilities in viscoelastic flows,” *Rheologica Acta* **31**, 213–263 (1992).
- [19] L. Pan, A. Morozov, C. Wagner, and P. E. Arratia, “Nonlinear elastic instability in channel flows at low reynolds numbers,” *Phys. Rev. Lett.* **110**, 174502 (2013).
- [20] A. Groisman and V. Steinberg, “Elastic vs. inertial instability in a polymer solution flow,” *Europhysics Letters* **43**, 165 (1998).
- [21] A. Groisman and V. Steinberg, “Elastic turbulence in a polymer solution flow,” *Nature* **405**, 53–55 (2000).
- [22] Alexander Groisman and Victor Steinberg, “Elastic turbulence in curvilinear flows of polymer solutions,” *New Journal of Physics* **6**, 29 (2004).
- [23] Boyang Qin and Paulo E. Arratia, “Characterizing elastic turbulence in channel flows at low reynolds number,” *Phys. Rev. Fluids* **2**, 083302 (2017).
- [24] Alexander Groisman and Victor Steinberg, “Efficient mixing at low reynolds numbers using polymer additives,” *Nature* **410**, 905–908 (2001).
- [25] S. Berti, A. Bistagnino, G. Boffetta, A. Celani, and S. Musacchio, “Two-dimensional elastic turbulence,” *Phys. Rev. E* **77**, 055306 (2008).
- [26] Samriddhi Sankar Ray and Dario Vincenzi, “Elastic turbulence in a shell model of polymer solution,” *Europhysics Letters* **114**, 44001 (2016).
- [27] Anupam Gupta and Dario Vincenzi, “Effect of polymer-stress diffusion in the numerical simulation of elastic turbulence,” *Journal of Fluid Mechanics* **870**, 405–418 (2019).
- [28] Yves Dubief, Vincent E. Terrapon, and Julio Soria, “On the mechanism of elasto-inertial turbulence,” *Physics of Fluids* **25** (2013).
- [29] Devranjan Samanta, Yves Dubief, Markus Holzner, Christof Schäfer, Alexander N. Morozov, Christian Wagner, and Björn Hof, “Elasto-inertial turbulence,” *Proceedings of the National Academy of Sciences* **110**, 10557–10562 (2013).
- [30] P. C. Valente, C. B. da Silva, and F. T. Pinho, “Energy spectra in elasto-inertial turbulence,” *Physics of Fluids* **28** (2016).
- [31] Yves Dubief, Vincent E. Terrapon, and Björn Hof, “Elasto-inertial turbulence,” *Annual Review of Fluid Mechanics* **55**, 675–705 (2023).
- [32] Wen-Hua Zhang, Hong-Na Zhang, Yu-Ke Li, Bo Yu, and Feng-Chen Li, “Role of elasto-inertial turbulence in viscoelastic drag-reducing turbulence,” *Physics of Fluids* **33** (2021).
- [33] KOLMOGOROV A. N., “Dissipation of energy in the locally isotropic turbulence,” *Dokl. Akad. Nauk. SSSR* **32**, 19–21 (1941).
- [34] U Frisch, *Turbulence: The Legacy of A. N. Kolmogorov* (Cambridge University Press, 1996).
- [35] Yi-Bao Zhang, Eberhard Bodenschatz, Haitao Xu, and Heng-Dong Xi, “Experimental observation of the elastic range scaling in turbulent flow with polymer additives,” *Science Advances* **7**, eabd3525 (2021).
- [36] Marco E. Rosti, Prasad Perlekar, and Dhruvaditya Mitra, “Large is different: Nonmonotonic behavior of elastic range scaling in polymeric turbulence at large reynolds and Deborah numbers,” *Science Advances* **9**, eadd3831 (2023).
- [37] Rahul K. Singh, Prasad Perlekar, Dhruvaditya Mitra, and Marco E. Rosti, “Intermittency in the not-so-smooth elastic turbulence,” (2023), [arXiv:2308.06997](https://arxiv.org/abs/2308.06997) [[physics.flu-dyn](https://arxiv.org/abs/2308.06997)].
- [38] Dario Vincenzi, Shi Jin, Eberhard Bodenschatz, and Lance R. Collins, “Stretching of polymers in isotropic turbulence: A statistical closure,” *Phys. Rev. Lett.* **98**, 024503 (2007).
- [39] F. De Lillo, G. Boffetta, and S. Musacchio, “Control of particle clustering in turbulence by polymer additives,” *Phys. Rev. E* **85**, 036308 (2012).
- [40] Faranggis Bagheri, Dhruvaditya Mitra, Prasad Perlekar, and Luca Brandt, “Statistics of polymer extensions in turbulent channel flow,” *Phys. Rev. E* **86**, 056314 (2012).
- [41] We use the ABC forcing to sustain the turbulent flow, such that $\mathbf{F} = \nu[(A \sin z + C \cos y) \hat{\mathbf{x}} + (B \sin x + A \cos z) \hat{\mathbf{y}} + (C \sin y + B \cos x) \hat{\mathbf{z}}]$, where $A = B = C = 1$.
- [42] See the Supplementary Materials for details.
- [43] Toshiyuki Gotoh, Takeshi Watanabe, and Izumi Saito, “Kinematic effects on probability density functions of energy dissipation rate and enstrophy in turbulence,” *Phys. Rev. Lett.* **130**, 254001 (2023).
- [44] Dhawal Buaria, Alain Pumir, Eberhard Bodenschatz,

- and P K Yeung, “Extreme velocity gradients in turbulent flows,” *New Journal of Physics* **21**, 043004 (2019).
- [45] Dhawal Buaria and Alain Pumir, “Vorticity-strain rate dynamics and the smallest scales of turbulence,” *Phys. Rev. Lett.* **128**, 094501 (2022).
- [46] Despite the mild variations in the ϵ_f -pdfs at different Re, the tails seem very likely to be stretched exponentials at all Re. However, this requires more analysis and data to obtain very clear and quantified conclusions.
- [47] Uriel Frisch, Pierre-Louis Sulem, and Mark Nelkin, “A simple dynamical model of intermittent fully developed turbulence,” *Journal of Fluid Mechanics* **87**, 719–736 (1978).
- [48] R Benzi, G Paladin, G Parisi, and A Vulpiani, “On the multifractal nature of fully developed turbulence and chaotic systems,” *Journal of Physics A: Mathematical and General* **17**, 3521 (1984).
- [49] Thomas C. Halsey, Mogens H. Jensen, Leo P. Kadanoff, Itamar Procaccia, and Boris I. Shraiman, “Fractal measures and their singularities: The characterization of strange sets,” *Phys. Rev. A* **33**, 1141–1151 (1986).
- [50] C. Meneveau and K.R. Sreenivasan, “The multifractal spectrum of the dissipation field in turbulent flows,” *Nuclear Physics B - Proceedings Supplements* **2**, 49–76 (1987).
- [51] K R Sreenivasan, “Fractals and multifractals in fluid turbulence,” *Annual Review of Fluid Mechanics* **23**, 539–604 (1991).
- [52] Charles Meneveau and K. R. Sreenivasan, “The multifractal nature of turbulent energy dissipation,” *Journal of Fluid Mechanics* **224**, 429–484 (1991).
- [53] R. Sureshkumar, Antony N. Beris, and Robert A. Handler, “Direct numerical simulation of the turbulent channel flow of a polymer solution,” *Physics of Fluids* **9**, 743–755 (1997).
- [54] J. K. Bhattacharjee and D. Thirumalai, “Drag reduction in turbulent flows by polymers,” *Phys. Rev. Lett.* **67**, 196–199 (1991).
- [55] D. Thirumalai and J. K. Bhattacharjee, “Polymer-induced drag reduction in turbulent flows,” *Phys. Rev. E* **53**, 546–551 (1996).
- [56] A. Fouxon and V. Lebedev, “Spectra of turbulence in dilute polymer solutions,” *Physics of Fluids* **15**, 2060–2072 (2003).
- [57] Adeel Ahmad and Dario Vincenzi, “Polymer stretching in the inertial range of turbulence,” *Phys. Rev. E* **93**, 052605 (2016).
- [58] T. Vaithianathan and Lance R. Collins, “Numerical approach to simulating turbulent flow of a viscoelastic polymer solution,” *Journal of Computational Physics* **187**, 1–21 (2003).
- [59] Anupam Gupta, Prasad Perlekar, and Rahul Pandit, “Two-dimensional homogeneous isotropic fluid turbulence with polymer additives,” *Phys. Rev. E* **91**, 033013 (2015).
- [60] M. Quan Nguyen, Alexandre Delache, Serge Simoëns, Wouter J. T. Bos, and Mamoud El Hajem, “Small scale dynamics of isotropic viscoelastic turbulence,” *Phys. Rev. Fluids* **1**, 083301 (2016).
- [61] Guido Boffetta, Antonio Celani, and Stefano Musacchio, “Two-dimensional turbulence of dilute polymer solutions,” *Phys. Rev. Lett.* **91**, 034501 (2003).
- [62] Yves Dubief, C. M. White, V. E. Terrapon, E. S. G. Shaqfeh, Parviz Moin, and S. K. Lele, “On the coherent drag-reducing and turbulence-enhancing behaviour of polymers in wall flows,” *Journal of Fluid Mechanics* **514**, 271–280 (2004).
- [63] Siddhartha Mukherjee, Sugan D. Murugan, Ritwik Mukherjee, and Samridhhi Sankar Ray, “Turbulent flows are not uniformly multifractal,” (2023), arXiv:2307.06074 [physics.flu-dyn].

Supplemental Material

Bridging Polymeric Turbulence at different Reynolds numbers: From Multiscaling to Multifractality

Rahul K. Singh^{1,*} and Marco E. Rosti^{1,†}

¹*Complex Fluids and Flows Unit, Okinawa Institute of Science and Technology Graduate University, Okinawa 904-0495, Japan*
(Dated: September 27, 2023)

NUMERICAL METHODS

We solve the fluid velocity and polymer conformation tensor field given by Eqns. 1(a) and 1(b) in the main text on a staggered, uniform, Cartesian grid using the in-house flow solver Fujin, which employs a second-order central finite difference scheme for spatial discretisation. Time marching for the velocity field is achieved via a second-order Adams-Bashforth scheme coupled with a fractional step method [1], while the non-Newtonian stress tensor is advanced in time via the Crank-Nicolson scheme. A log-conformation formulation [2] ensures positive-definiteness of the conformation tensor at all times. Obtaining incompressible fluid velocity at each time requires solving a Poisson equation for pressure, which is done using a solver based on Fast Fourier Transform (FFT). The solver is parallelized using the domain decomposition library 2decomp and the MPI protocol.

We solve the equations on a $2\pi \times 2\pi \times 2\pi$ -periodic domain that is discretized into $N^3 = 1024^3$ points. We choose two different time-steppings of $\delta t = 1.25 \times 10^{-5}$ and $\delta t = 2.5 \times 10^{-5}$ for small and large Re_λ simulations, which respectively equal $1.5 \times 10^{-3}\tau_\eta$ and $2 \times 10^{-3}\tau_\eta$, where τ_η is the Kolmogorov time-scale. Similarly, the smallest spatial scales resolved are equal to 0.05η and η for the smallest and largest Re_λ simulations. Field data is saved every 2×10^4 time steps for data analysis.

POLYMER SPECTRA

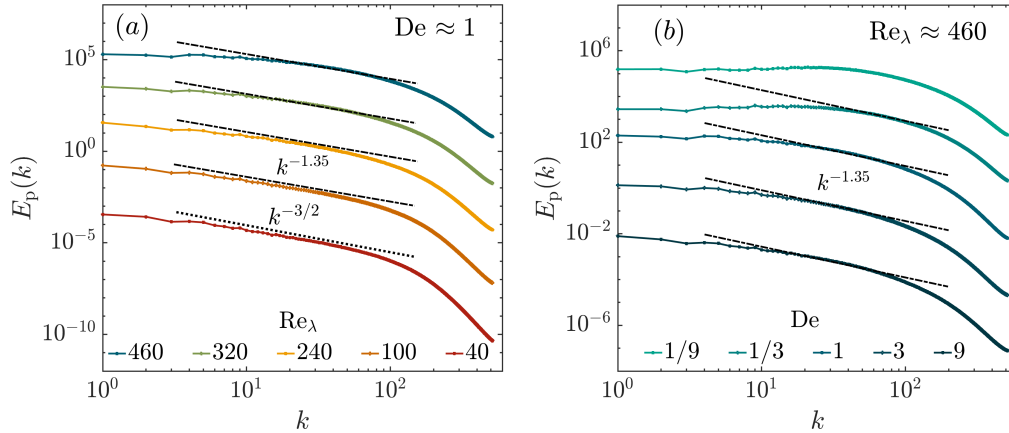


FIG. 1. The dependence of the polymer energy spectrum $E_p(k)$ on (a) Re (shown for $\text{De} \approx 1$), and on (b) De (shown for $\text{Re}_\lambda \approx 460$). The two different scaling regimes with exponents -1.35 (at large Re) and -1.5 (at small Re) are shown in dash-dotted and dotted lines, respectively. (b) Small De flows at large Re show a close to Newtonian behaviour and $E_p(k)$ remains devoid of any scaling form. As $\text{De} \gtrsim 1$, the expected scaling with exponent -1.35 begins to appear.

The polymer energy spectrum $E_p(k)$ can be defined using the positive-definite square root \mathbf{B} (with components B_{ij}) of the conformation tensor \mathbf{C} , i.e. $C_{ij} = B_{ik}B_{kj}$.

$$E_p(k) = \frac{\mu_p}{2\tau_p} \int d\mathbf{q} \langle B_{ij}(-\mathbf{q})B_{ji}(\mathbf{q}) \rangle \delta(|\mathbf{q}| - k). \quad (1)$$

We can estimate $E_p(k)$ by using appropriate scaling arguments in different regimes. Assume that velocity and polymer fields transform under scaling as $u \rightarrow \lambda^h u$, $C \rightarrow \lambda^g C$, when spatial separations scale as $r \rightarrow \lambda r$, where h and g are undetermined constants [3]. Clearly, the Fourier transformed variables scale as $u_k \sim k^{-h}$, $C_k \sim k^{-g}$. Energy in a scale k can be approximated as $kE_k \sim u_k^2 \sim k^{-2h}$ and $kE_{pk} \sim C_k \sim k^{-g}$. At large Re, $E_k \sim k^{-2h-1} = k^{-2.3}$ implies $h \approx 0.65$ in the polymer range. Similarly, an approximately constant Π_p in Fig. 2(a) of the main text means $ku_k C_k \sim k^0$ yielding $g + h = 1$. Thus, $E_{pk} \sim k^{-g-1} = k^{h-2} = k^{-1.35}$. This is found to be true for moderate and large Re in Fig. 1(a).

At small Re, dissipative effects become important and both \mathcal{D}_p and \mathcal{D}_f are of the same order for $\forall k \gtrsim 10$ in Fig. 2(c) of main text. So, we simply compare the two viscous terms [4]:

$$k^2 u_k^2 \sim k u_k C_k \Rightarrow E_{pk} \sim \sqrt{k E_k} = k^{-3/2}, \quad (2)$$

where we have used $E_k \sim k^{-4}$ at small Re. Indeed, this is consistent with the observations from simulations as shown in Fig. 1(a). We find that $E_p(k) \sim k^{-3/2}$ when $\text{Re}_\lambda \approx 40$. Admittedly, the two slopes -1.35 and -1.5 are very close and may as well be indistinguishable but are both consistent with the respective scaling predictions.

In Fig. 1(b), we show how $E_p(k)$ changes with polymer elasticity at large Re. Again, the cleanest scaling range appears when elasticity is large, as the polymers extend to much larger lengths giving a self-similar distribution of polymer energy over a wide range of scales.

FLUXES

In this section, we describe how various flux contributions in Eqn. 2 of the main text are computed. We begin with the modified Navier-Stokes Eqn. 1(a) (of the main text):

$$\partial_t \mathbf{u} + \mathbf{u} \cdot \nabla \mathbf{u} = -\nabla p + \nu \nabla^2 \mathbf{u} + \frac{\mu_p}{\rho \tau_p} \nabla \cdot \mathbf{C} + \mathbf{F}, \quad \nabla \cdot \mathbf{u} = 0. \quad (3)$$

To obtain the individual fluxes, we first Fourier transform Eqn. 3,

$$\partial_t \hat{u}_i(\mathbf{k}) + \mathcal{N}_i(\mathbf{k}) = ik_i \hat{p} - \nu k^2 \hat{u}_i(\mathbf{k}) + \frac{\mu_p}{\rho \tau_p} ik_j \hat{C}_{ij} + \hat{F}_i(\mathbf{k}), \quad k_i \hat{u}_i = 0; \quad i, j = 1, 2, 3, \quad (4)$$

where the hat $\hat{\cdot}$ denotes the Fourier transformed variables and $\mathcal{N}_i(\mathbf{k})$ is the Fourier transform of the non-linear term. Summation over repeated indices is implied. Taking the complex conjugate of the above equation we obtain

$$\partial_t \hat{u}_i^*(\mathbf{k}) + \mathcal{N}_i^*(\mathbf{k}) = -ik_i \hat{p}^* - \nu k^2 \hat{u}_i^*(\mathbf{k}) - \frac{\mu_p}{\rho \tau_p} ik_j \hat{C}_{ij}^* + \hat{F}_i^*(\mathbf{k}). \quad (5)$$

The energy equation for any k -th mode can be obtained by multiplying Eqn. 4 by $u_i^*(\mathbf{k})$, Eqn. 5 by $u_i(\mathbf{k})$, and adding them:

$$\partial_t \mathcal{E}(\mathbf{k}) + \text{Re}\{\hat{u}_i^*(\mathbf{k}) \mathcal{N}_i(\mathbf{k})\} = -\nu k^2 |\hat{u}_i(\mathbf{k})|^2 + \frac{\mu_p}{\rho \tau_p} \text{Im}\{\hat{u}_i^*(\mathbf{k}) k_j \hat{C}_{ij}\} + \text{Re}\{\hat{u}_i^*(\mathbf{k}) \hat{F}_i(\mathbf{k})\}, \quad (6)$$

where $\mathcal{E}(\mathbf{k}) = |u_i(\mathbf{k})|^2/2$ is the energy in mode \mathbf{k} , the pressure term vanishes away due to incompressibility, and $\text{Re}\{\cdot\}$ and $\text{Im}\{\cdot\}$ denote the real and imaginary parts respectively. The total energy flux from modes $k < K$ to modes $k > K$ can be obtained by integrating from 0 to K :

$$\begin{aligned} \partial_t \int_0^K d\mathbf{k} \mathcal{E}(\mathbf{k}) + \int_0^K d\mathbf{k} \text{Re}\{\hat{u}_i^*(\mathbf{k}) \mathcal{N}_i(\mathbf{k})\} = \\ -\nu \int_0^K d\mathbf{k} k^2 |\hat{u}_i(\mathbf{k})|^2 + \frac{\mu_p}{\rho \tau_p} \int_0^K d\mathbf{k} \text{Im}\{\hat{u}_i^*(\mathbf{k}) k_j \hat{C}_{ij}\} + \int_0^K d\mathbf{k} \text{Re}\{\hat{u}_i^*(\mathbf{k}) \hat{F}_i(\mathbf{k})\}. \end{aligned} \quad (7)$$

In a statistically stationary state, the total energy in any set of modes is a constant, so that $\partial_t \int_0^K d\mathbf{k} \mathcal{E}(\mathbf{k}) = 0$. Choosing suitable symbols for the remaining terms, we have:

$$\Pi_f'(K) = -\mathcal{D}_f'(K) + \mathcal{P}'(K) + \mathcal{F}(K), \quad (8)$$

where Π'_f , \mathcal{D}'_f , \mathcal{P}' , and \mathcal{F} are the contributions from fluid non-linearity, fluid dissipation, polymer stresses, and the external forcing term respectively. Since the forcing is applied at only $K = 1$, we have for any $K \geq 1$:

$$\Pi'_f(K) + \mathcal{D}'_f(K) - \mathcal{P}'(K) = \mathcal{F}(K) = \epsilon_t, \quad (9)$$

where ϵ_t is the rate of total energy injection into the system by the forcing \mathbf{F} . Thus, upon normalization by ϵ_t , we have:

$$\Pi_f(K) + \mathcal{D}_f(K) + \mathcal{P}(K) = 1, \quad (10)$$

where $\Pi_f = \Pi'_f/\epsilon_t$, $\mathcal{D}_f = \mathcal{D}'_f/\epsilon_t$, $\mathcal{P} = -\mathcal{P}'/\epsilon_t$. We plot the curves for Π_f , \mathcal{D}_f , and \mathcal{P} in Fig. 2 of the main text.

VELOCITY GRADIENTS

We showed in the main text how the statistics of fluid energy dissipation rate ϵ_f depend on Re and De. We now discuss in detail how do varying fluid inertia (Re) and polymer elasticity (De) result in different extreme statistics of $\epsilon_f = 2\nu S_{ij}S_{ij} = 2\nu[(\partial_i u_j + \partial_j u_i)/2]^2$. To this end, we look at how the velocity gradients $\partial_i u_j$ themselves evolve. Their governing equations can be obtained by taking the gradient of Eqn. 1(a) in the main text. Denoting the gradients by $\mathbf{A} = \nabla \mathbf{u}$, we obtain:

$$\partial_t \mathbf{A} = -\mathbf{A}^2 - \mathbf{u} \cdot \nabla \mathbf{A} - \mathbf{H}^p + \nu \nabla^2 \mathbf{A} + \frac{\nu}{9\tau_p} \mathbf{H}^C, \quad (11)$$

$$\partial_t \mathbf{C} = -\mathbf{u} \cdot \nabla \mathbf{C} + \mathbf{C} \mathbf{A} + \mathbf{A}^T \mathbf{C} + \frac{1}{\tau_p} (\mathbf{I} - \mathbf{C}). \quad (12)$$

where $\mathbf{H}^p = \partial_i \partial_j p$ and $\mathbf{H}^C = \partial_i \partial_k C_{kj}$ denote the pressure and conformation Hessians respectively.

Let us begin our discussion with large Re ($\text{Re}_\lambda \approx 460$). For small De, eqn. 12 just implies $\mathbf{C} = \mathbf{I}$. This is seen easily by multiplying Eqn. 12 with τ_p and taking the limit $\tau_p \rightarrow 0$. Polymers are, thus, minimally stretched at small De, and the fluctuations in \mathbf{C} are rather small. Consequently, the conformation Hessian \mathbf{H}^C remains small compared to the other terms in Eqn. 11 and we get a close to Newtonian behaviour at small De.

In contrast, to see what happens at large De, we need to estimate the individual contributions of the different terms in Eqn. 11. For simplicity, the typical estimates are now denoted without the bold notation. We recall from the main text that the fluid energy spectrum is marked by three distinct regimes at large De (and large Re) with the spectrum exponent δ , where $E(k) \sim k^{-\delta}$, given as:

$$\delta = \begin{cases} 5/3, & k \text{ small,} \\ 2.3, & k \text{ intermediate,} \\ > 4, & k \text{ large.} \end{cases} \quad (13)$$

This means velocity fluctuations u_l in the corresponding ranges scale as $u_l \sim l^{\zeta_1}$, where:

$$\zeta_1 = \begin{cases} 1/3, & l \text{ large,} \\ 0.65, & l \text{ intermediate,} \\ 1, & l \text{ small.} \end{cases} \quad (14)$$

We obtain ζ_1 by noting that the exponents ζ_2 for squared velocity fluctuations, $u_l^2 \sim l^{\zeta_2}$, are related to δ as $\zeta_2 = \delta - 1$ for $\delta \leq 3$ [5]. For any $\delta > 3$, we have instead $\zeta_2 = 2$ [6, Appendix G]. The exponents ζ_1 are then obtained as $\zeta_1 = \zeta_2/2 = (\delta - 1)/2$ for $\delta \leq 3$ and $\zeta_1 = 1$ for $\delta > 3$, i.e. we ignore corrections due to intermittency for this analysis. Denoting the largest length and velocity scales by l_0 and u_0 respectively, fluctuations at successively smaller scales can be estimated as:

$$\begin{aligned} u_l &\sim u_0 \left(\frac{l}{l_0}\right)^{1/3}, & l_a \leq l \leq l_0, \\ u_l &\sim u_a \left(\frac{l}{l_a}\right)^{0.65} \approx u_a \left(\frac{l}{l_a}\right)^{2/3}, & l_b \leq l \leq l_a, \\ u_l &\sim u_b \frac{l}{l_b}, & l \leq l_b, \end{aligned}$$

where $u_{a/b}$ are typical velocity fluctuations at the crossover scales $l_{a/b}$. The typical velocity gradients A can be written as rescaled velocity fluctuations at the smallest scale l :

$$A \sim \frac{u_l}{l} \sim u_b \frac{1}{l_b} \sim u_a \left(\frac{l_b}{l_a}\right)^{2/3} \frac{1}{l_b} \sim u_0 \left(\frac{l_a}{l_0}\right)^{1/3} \left(\frac{l_b}{l_a}\right)^{2/3} \frac{1}{l_b} = \frac{u_0}{(l_0 l_a l_b)^{1/3}}. \quad (15)$$

These typical estimates for velocity gradients do not take into account constants of $\mathcal{O}(1)$, therefore, they can only be used to compare relative contributions from extreme events (or tails of dissipation pdfs). This is exactly what concerns us: how do the tails of ϵ_f -pdfs differ between Newtonian and polymeric flows at different Re.

In a similar vein, one can obtain real space scaling relations for polymer conformation fluctuations using the exponents for polymer spectra $E_p(k)$ plotted in Fig. 1. The relation between scaling exponents $C_l \sim l^\xi$ for polymer fluctuations and polymer spectra $E_p(k) \sim k^{-\gamma}$ is found to be $\xi = \gamma - 1$ [4, and main text] for $\gamma \leq 3$ and $\xi = 2$ for $\gamma > 3$. We use $De \approx 9$ for the following estimates at large Re. From Fig. 1(b), $E_p(k)$ admits two scaling ranges with slopes -1.35 and -5 . Therefore:

$$\begin{aligned} C_l &\sim C_0 \left(\frac{l}{l_0}\right)^{0.35} \approx C_0 \left(\frac{l}{l_0}\right)^{1/3}, & l_b \leq l \leq l_0, \\ C_l &\sim C_b \left(\frac{l}{l_b}\right)^2, & l \leq l_b. \end{aligned} \quad (16)$$

The typical second derivatives H^C of polymer conformation are found to be:

$$H^C \sim \frac{C_l}{l^2} \sim \frac{C_b}{l_b^2} \sim C_0 \left(\frac{l_b}{l_0}\right)^{1/3} \frac{1}{l_b^2} = \frac{C_0}{(l_0 l_b^5)^{1/3}}. \quad (17)$$

The inviscid fluid contributions compared to the polymer term can be estimated as:

$$\begin{aligned} \frac{A^2}{\nu H^C / 9\tau_p} &\sim \frac{u_0^2 / (l_0 l_a l_b)^{2/3}}{(\nu C_0 / 9\tau_p) (1/l_b^5 l_0)^{1/3}} = \frac{9\tau_p u_0^2}{\nu C_0} \left(\frac{l_b^3}{l_0 l_a^2}\right)^{1/3} \sim \mathcal{O}(1), \\ \frac{u \nabla A}{\nu H^C / 9\tau_p} &\sim \frac{u_0^2 / l (l_0 l_a l_b)^{1/3}}{(\nu C_0 / 9\tau_p) (1/l_b^5 l_0)^{1/3}} = \frac{9\tau_p u_0^2}{\nu C_0} \left(\frac{l_b^4}{l^3 l_a}\right)^{1/3} \sim \mathcal{O}(10^2), \end{aligned}$$

where we have used $l_a \approx l_0/6$, $l_b \approx l_0/80$ (cf. Fig. 1(c), main text), and $l/l_0 = 512$. The factor $9\tau_p u_0^2 / \nu C_0 \approx 60$ comes from our simulation results. We have also approximated $u \nabla A$ by treating the gradient field as being passively advected by the large scale motions of the flow. Clearly, the polymer contribution is negligible compared to the fluid self-interactions which remain the dominant contributor to extreme, intermittent events. As a result, the tails of dissipation pdfs at large Re remain independent of elasticity.

We now turn our attention to when Re is very small, i.e. $Re_\lambda \approx 40$. The velocity fields are now smooth and the fluctuations scale, to the leading order, as $u_l \sim l/l_0$ [4]. The velocity gradients thus scale as $A \sim u_l/l \sim u_0/l_0$. From Fig. 1(a), when $De \approx 1$, the polymer spectra at small Re comprises two scaling ranges: $E_p(k) \sim k^{-3/2}$ for $k_b \geq k \geq k_0$ and $E_p(k) \sim k^{-\delta}$ with $\delta > 3$ for $k > k_b$. This means polymer fluctuations scale as $C_l \sim l^{1/2}$ for $l_b \leq l \leq l_0$ and $C_l \sim l^2$ for $l \leq l_b$. Thus,

$$C_l \sim C_0 \left(\frac{l}{l_b}\right)^2 \left(\frac{l_b}{l_0}\right)^{1/2} \Rightarrow H^C \sim \frac{C_l}{l^2} \sim \frac{C_0}{(l_b^3 l_0)^{1/2}}. \quad (18)$$

The various terms can now be readily compared

$$\begin{aligned} \frac{\nu H^C / 9\tau_p}{A^2} &\sim \frac{(\nu C_0 / 9\tau_p) / (l_b^3 l_0)^{1/2}}{u_0^2 / l_0^2} = \frac{\nu C_0}{9\tau_p u_0^2} \left(\frac{l_0}{l_b}\right)^{3/2} \sim \mathcal{O}(10^2), \\ \frac{\nu H^C / 9\tau_p}{u \nabla A} &\sim \frac{(\nu C_0 / 9\tau_p) / (l_b^3 l_0)^{1/2}}{u_0^2 / l_0 l} = \frac{\nu C_0}{9\tau_p u_0^2} \frac{l}{l_b} \left(\frac{l_0}{l_b}\right)^{1/2} \sim \mathcal{O}(1). \end{aligned}$$

We have again used $l_b \approx l_0/80$, and $l/l_0 = 512$. We have used $\nu C_0 / 9\tau_p u_0^2 \approx 0.32$ taken from simulations when $Re_\lambda \approx 40$. Clearly, the polymer contributions to the time-evolution of velocity gradients can no longer be ignored

as they are the same order as the fluid terms. Hence, when Re is small, fluctuations in polymer lengths with large elasticity can create strong fluctuations in the carrier fluid velocity. These fluctuations then result in strong gradients. Consequently, ϵ_f -pdfs develop long right tails as seen in Fig. 3 in the main text.

* rksphys@gmail.com

† marco.rosti@oist.jp

- [1] J. Kim and P. Moin, *Journal of Computational Physics* **59**, 308 (1985).
- [2] D. Izbassarov, M. E. Rosti, M. N. Ardekani, M. Sarabian, S. Hormozi, L. Brandt, and O. Tammisola, *International Journal for Numerical Methods in Fluids* **88**, 521.
- [3] M. E. Rosti, P. Perlekar, and D. Mitra, *Science Advances* **9**, eadd3831 (2023).
- [4] R. K. Singh, P. Perlekar, D. Mitra, and M. E. Rosti, “Intermittency in the not-so-smooth elastic turbulence,” (2023), arXiv:2308.06997 [physics.flu-dyn].
- [5] U. Frisch, *Turbulence: The Legacy of A. N. Kolmogorov* (Cambridge University Press, 1996).
- [6] S. Pope, *Turbulence* (Cambridge University Press, Cambridge, 2000).